

## 2 Soil water flow

*J.C. van Dam, R.A. Feddes*

### 2.1 Basic equations

Spatial differences of the soil water potential induce soil water movement. Darcy's equation is commonly used to quantify these soil water fluxes. For one-dimensional vertical flow, Darcy's equation can be written as:

$$q = -K(h) \frac{\partial(h+z)}{\partial z} \quad (2.1)$$

where  $q$  is soil water flux density (positive upward) ( $\text{cm d}^{-1}$ ),  $K$  is hydraulic conductivity ( $\text{cm d}^{-1}$ ),  $h$  is soil water pressure head (cm) and  $z$  is the vertical coordinate (cm), taken positively upward.

Water balance considerations of an infinitely small soil volume result in the continuity equation for soil water:

$$\frac{\partial \theta}{\partial t} = -\frac{\partial q}{\partial z} - S_a(h) \quad (2.2)$$

where  $\theta$  is volumetric water content ( $\text{cm}^3 \text{cm}^{-3}$ ),  $t$  is time (d) and  $S_a$  is soil water extraction rate by plant roots ( $\text{cm}^3 \text{cm}^{-3} \text{d}^{-1}$ ).

Combination of Eqs. (2.1) and (2.2) provides the general water flow equation in variably saturated soils, known as the Richards' equation:

$$\frac{\partial \theta}{\partial t} = C(h) \frac{\partial h}{\partial t} = \frac{\partial \left[ K(h) \left( \frac{\partial h}{\partial z} + 1 \right) \right]}{\partial z} - S_a(h) \quad (2.3)$$

where  $C$  is the water capacity ( $\partial\theta/\partial h$ ) ( $\text{cm}^{-1}$ ).

Richards' equation has a clear physical basis at a scale where the soil can be considered to be a continuum of soil, air and water. SWAP solves Eq. (2.3) numerically, subject to specified initial and boundary conditions and with known relations between  $\theta$ ,  $h$  and  $K$ . These relationships can be measured directly in the soil, determined in the laboratory, or might be obtained from basic soil data as discussed in Par. 3.2. SWAP applies Richards' equation integrally for the unsaturated-saturated zone, including possible transient and perched groundwater levels.

### 2.2 Numerical solution of soil water flow equation

Accurate numerical solution of Richards' partial differential equation is not easy due to its hyperbolic nature, the strong non-linearity of the soil hydraulic functions and the rapid

changing boundary conditions near the soil surface. In the past calculated soil water fluxes could be significantly affected by the structure of the numerical scheme, the applied time and space discretizations, and the procedure for the top boundary condition (Van Genuchten, 1982; Milly, 1985; Celia et al., 1990; Warrick, 1991; Zaidel and Russo, 1992). In SWAP a numerical scheme has been chosen which solves the one-dimensional Richards' equation with an accurate mass balance and which converges rapidly. This scheme in combination with the top boundary procedure has been shown to handle rapid soil water movement during infiltration in dry soils accurately. At the same time the scheme is fast, calculating periods of 40-70 years in a few minutes (Van Dam and Feddes, 2000).

### 2.2.1 Numerical discretization in the soil profile

A common method to solve Richards' equation has been the implicit, backward, finite difference scheme with explicit linearization as described by Haverkamp et al. (1977) and Belmans et al. (1983). Three adaptations to this scheme were made to arrive at the numerical scheme currently applied in SWAP. The first adaptation concerns the handling of the differential water capacity  $C$ . The old scheme was limited to the unsaturated zone only. The saturated zone and fluctuations of the groundwater table had to be modelled separately (Belmans et al., 1983). The new numerical scheme enables us to solve the flow equation in the unsaturated and saturated zone simultaneously. In order to do so, in the numerical discretization of Richards' equation, the  $C$ -term only occurs as numerator, not as denominator (see Eq. (2.3)).

The second adaptation concerns the numerical evaluation of the  $C$ -term. Because of the high non-linearity of  $C$ , averaging during a time step results in serious mass balance errors when simulating highly transient conditions. A simple but effective adaptation was suggested by Milly (1985) and further analysed by Celia et al. (1990). Instead of applying during a *time* step

$$\theta_i^{j+1} - \theta_i^j = C_i^{j+1/2} (h_i^{j+1} - h_i^j) \quad (2.4)$$

where  $C_i^{j+1/2}$  denotes the average water capacity during the time step, subscript  $i$  is the node number (increasing downward) and superscript  $j$  is the time level, they applied at each *iteration* step:

$$\theta_i^{j+1} - \theta_i^j = C_i^{j+1,p-1} (h_i^{j+1,p} - h_i^{j+1,p-1}) + \theta_i^{j+1,p-1} - \theta_i^j \quad (2.5)$$

where superscript  $p$  is the iteration level and  $C_i^{j+1,p-1}$  is the water capacity evaluated at the  $h$  value of the last iteration. At convergence  $(h_i^{j+1,p} - h_i^{j+1,p-1})$  will be small, which eliminates effectively remaining inaccuracies in the evaluation of  $C$ .

The third adaptation concerns the averaging of  $K$  between the nodes. Haverkamp and Vauclin (1979), Belmans et al. (1983) and Hornung and Messing (1983) proposed to use the geometric mean. In their simulations the geometric mean increased the accuracy of calculated fluxes and caused the fluxes to be less sensitive to changes in nodal distance. However, the geometric mean has serious disadvantages too (Warrick, 1991). When simulating infiltration in dry soils or high evaporation from wet soils, the geometric mean severely underestimates the water fluxes. Other researchers proposed to use the harmonic mean of  $K$  or various kind of weighted averages (Ross, 1990; Warrick, 1991; Zaidel and Russo, 1992; Desbarats, 1995). Van Dam and Feddes (2000) show that, although arithmetic

averages at larger nodal distances overestimate the soil water fluxes in case of infiltration and evaporation events, at nodal distances in the order of 1 cm arithmetic averages are more close to the theoretically correct solution than geometric averages. Also they show that the remaining inaccuracy between calculated and theoretically correct fluxes, is relatively small compared to effects of soil spatial variability and hysteresis. Therefore SWAP applies arithmetic averages of  $K$ , which is in line with commonly applied finite element models (Kool and Van Genuchten, 1991; Šimůnek et al., 1992).

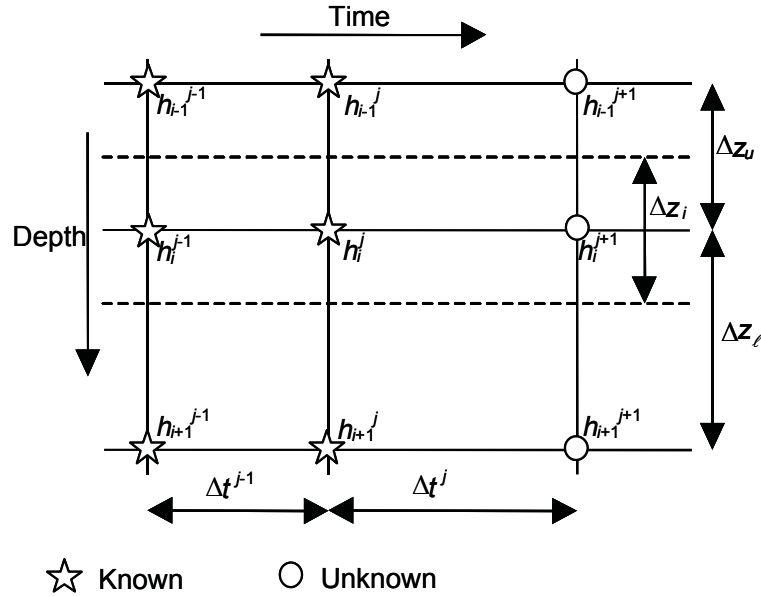


Figure 3 Spatial and temporal discretization used to solve Richards' equation

The implicit, backward, finite difference scheme of Eq. (2.3) with explicit linearization, including the three adaptations, yields the following discretization of Richards' equation:

$$C_i^{j+1,p-1} (h_i^{j+1,p} - h_i^{j+1,p-1}) + (\theta_i^{j+1,p-1} - \theta_i^j) = \frac{\Delta t^j}{\Delta z_i} \left[ K_{i-1/2}^j \left( \frac{h_{i-1}^{j+1,p} - h_i^{j+1,p}}{\Delta z_u} \right) + K_{i-1/2}^j - K_{i+1/2}^j \left( \frac{h_i^{j+1,p} - h_{i+1}^{j+1,p}}{\Delta z_\ell} \right) - K_{i+1/2}^j \right] - \Delta t^j S_i^j \quad (2.6)$$

where  $\Delta t^j = t^{j+1} - t^j$ ,  $\Delta z_u = z_{i-1} - z_i$ ,  $\Delta z_\ell = z_i - z_{i+1}$  and  $\Delta z_i$  is compartment thickness. Figure 3 shows the symbols in the space-time domain.  $K$  and  $S$  are evaluated at the old time level  $j$  (explicit linearization), which can be shown to give a good approximation at the time steps used. This numerical scheme applies both to the saturated and unsaturated zone. Starting in the saturated zone, the groundwater table is simply found at  $h = 0$ . Also perched water tables may occur above dense layers in the soil profile. Calculations show that in order to simulate infiltration and evaporation accurately, near the soil surface the nodal distance should be in the order of centimetres. For this reason the nodal distance in SWAP is made variable. Application of Eq. (2.6) to each node, subject to the prevailing boundary conditions, results in a tri-diagonal system of equations which can be solved efficiently (Press et al., 1989).

In the past the pressure head difference  $|h_i^{j+1,p} - h_i^{j+1,p-1}|$  in the iterative solution of Eq. (2.6) has been used as convergence criterium. Instead Huang et al. (1996) proposed to use the water content difference  $|\theta_i^{j+1,p} - \theta_i^{j+1,p-1}|$ . The advantage of a criterium based on  $\theta$  is that it is automatically more sensitive in pressure head ranges with a large differential soil water capacity,  $C=(d\theta/dh)$ , while it allows less iterations at low  $h$ -values where  $\theta$  hardly changes. Huang et al. (1996) show the higher efficiency of the  $\theta$ -criterium for a large number of infiltration problems. Moreover the  $\theta$ -criterium was found to be more robust when the soil hydraulic characteristics were extremely non-linear. Therefore in SWAP the main convergence criterium in the unsaturated zone is based on the water content difference  $|\theta_i^{j+1,p} - \theta_i^{j+1,p-1}|$ . In saturated or near-saturated compartments the  $\theta$ -criterium is insensitive, therefore SWAP uses in addition a maximum of the pressure head difference  $|h_i^{j+1,p} - h_i^{j+1,p-1}|$ .

The optimal time step should minimize the computational effort of a simulation while the numerical solution still meets the convergence criteria mentioned above. The number of iterations needed to reach convergence,  $N_{it}$ , can effectively be used for this purpose (Kool and Van Genuchten, 1991). In SWAP the following criteria are applied:

$N_{it} < 2$  : multiply time step with a factor 1.25  
 $2 \leq N_{it} \leq 4$  : keep time step the same  
 $N_{it} > 4$  : divide time step by a factor 1.25

In the SWAP input file a minimum and a maximum time step,  $\Delta t_{min}$  and  $\Delta t_{max}$  (d), are defined. For the initial time step, SWAP will take  $\Delta t = \sqrt{\Delta t_{min}\Delta t_{max}}$ . Depending on  $N_{it}$ , the time step will be decreased, maintained or increased for the following timesteps. If during an iteration  $N_{it}$  exceeds 6, SWAP will divide  $\Delta t$  by a factor 3, and start iterating again. The timestep is always confined to the range  $\Delta t_{min} \leq \Delta t \leq \Delta t_{max}$ . Exceptions to above procedure occur, when the upper boundary flux changes from evaporation to intensive rainfall ( $> 1.0 \text{ cm d}^{-1}$ ), in which case  $\Delta t$  is reset to  $\Delta t_{min}$ , and at the end of a day, in which case  $\Delta t$  is set equal to the remaining time in the day.

In some application it is known that large fluctuations in the groundwater level do not occur. An input parameter (GWLCONV) may be used to influence the convergence process and prevent large fluctuations in groundwater levels. However, when the model is applied under frost conditions, this input parameters can best be set to a high value (e.g. 500 cm) because groundwater levels in frozen soils (permafrost) are inaccurate and should not be used to influence the iteration scheme.

For some applications the accuracy of the water balance requires critical values. For this purpose the absolute deviation in the water balance is determined during each timestep and the iteration process continues until a given critical values is achieved. This critical value (CritDevMasBalDt) is input to the model.



In Figure 4 criterium <1> refers to whether the soil is saturated. If so, criterium <2> determines whether the soil is still saturated at the next time level  $t^{j+1}$  or becomes unsaturated. The inflow  $Q_{in}$  (cm) is defined as:

$$\begin{aligned} Q_{in} &= (q_{bot} - q_{top} - q_{root} - q_{drain}) \Delta t^j & \text{if } q_{top} > I_{max} \\ Q_{in} &= (q_{bot} - I_{max} - q_{root} - q_{drain}) \Delta t^j & \text{if } q_{top} < I_{max} \end{aligned} \quad (2.7)$$

where  $q_{bot}$  is the flux at the soil profile bottom (cm d<sup>-1</sup>),  $q_{top}$  the potential flux at the soil surface (cm d<sup>-1</sup>),  $q_{drain}$  the flux to drains or ditches (cm d<sup>-1</sup>) and  $I_{max}$  is the maximum infiltration rate (cm d<sup>-1</sup>). The potential flux at the soil surface  $q_{top}$  follows from:

$$q_{top} = q_{eva} - q_{prec} - q_{irrig} - q_{melt} - q_{runon} - \frac{h_{pond}}{\Delta t^j} \quad \text{with } q_{top} \geq I_{max} \quad (2.8)$$

where  $q_{eva}$  is the actual soil evaporation (cm d<sup>-1</sup>),  $q_{prec}$  is the precipitation at the soil surface (cm d<sup>-1</sup>),  $q_{irrig}$  is the irrigation at the soil surface (cm d<sup>-1</sup>),  $q_{melt}$  is the melt water flux from the snowpack (cm d<sup>-1</sup>) (paragraph 3.2),  $q_{runon}$  is the runoff (cm d<sup>-1</sup>) (paragraph 4.1.2) and  $h_{pond}$  is the height of water ponding on the soil surface (cm).

Criterium <3> determines whether the soil becomes or remains unsaturated. If the soil becomes unsaturated, criterium <3a>, a distinction is made between evaporation and infiltration. In case of evaporation, criterium <4>, the maximum flux is limited to the maximum flux according to Darcy,  $E_{max}$  (cm d<sup>-1</sup>):

$$E_{max} = K_{\frac{1}{2}} \left( \frac{h_{atm} - h_1^{j+1,p-1} - z_1}{z_1} \right) \quad (2.9)$$

with  $h_{atm}$  (cm) the soil water pressure head in equilibrium with the prevailing air relative humidity:

$$h_{atm} \approx -2.75 \cdot 10^5 \text{ cm} \quad (2.10)$$

In the case of infiltration (criterium <5>) a head-controlled condition applies if the potential flux  $q_{top}$  exceeds the maximum infiltration rate  $I_{max}$  and the saturated hydraulic conductivity  $K_{sat}$ .  $I_{max}$  (cm d<sup>-1</sup>) is calculated as:

$$I_{max} = K_{\frac{1}{2}} \left( \frac{h_{pond} - h_1^{j+1,p-1} - z_1}{z_1} \right) \quad (2.11)$$

The average hydraulic conductivity ( $K_{\frac{1}{2}}$ ) is calculated with the saturated hydraulic conductivity and, in the case of a frozen soil, a correction factor for the soil temperature (Eq.(2.28) and (2.29)).

When the soil is unsaturated, criterium <6> determines if the soil will be saturated at the next time level  $t^{j+1}$  (head is prescribed) or if the soil remains unsaturated. The symbol  $V_{air}$  (cm) denotes the pore volume in the soil profile being filled with air at time level  $t^j$  (see also

Eq. (2.30). If the soil remains unsaturated, criterium <3b>, a distinction is made between evaporation, criterium <4b>, and infiltration.

In case of infiltration, criterium <7>, the difference between the saturated and actual water content determines if the infiltration capacity of the soil is sufficient for the infiltration flux. During the iteration, when no convergence is reached, it might be possible that the actual water content is higher than the saturated water content. For criterium <8> the maximum infiltration capacity of the soil profile ( $I_{\max, \text{prof}}$ ) is calculated:

$$I_{\max, \text{prof}} = \frac{-q_{\text{top}} \sum_{i=1}^m z_i}{\sum_{i=1}^m K_i + \sum_{i=1}^m z_i} \quad (2.12)$$

where  $m$  is the number of soil compartments with a total  $V_{\text{air}}$  smaller than  $Q_{\text{in}}$ ,  $z_i$  is the depth of soil compartment  $i$  and  $K_i$  is the conductivity of soil compartment  $i$ .

During the iterative procedure of calculating  $h_i^{j+1, p}$  from the tri-diagonal system of equations (Par. 2.2.1), the top boundary condition is updated at each iteration  $p$ . Therefore the runoff and depth of the ponding layer are also recalculated as described in paragraph 4.1

### 2.2.3 Actual soil evaporation

In the case of a wet soil, soil evaporation is determined by the atmospheric demand and equals potential soil evaporation rate  $E_p$ . When the soil becomes drier, the soil hydraulic conductivity decreases, which may reduce  $E_p$  to a lower actual evaporation rate,  $E_a$  ( $\text{cm d}^{-1}$ ). In SWAP the maximum evaporation rate which the top soil may deliver,  $E_{\max}$  ( $\text{cm d}^{-1}$ ), is calculated according to Darcy's law (see also Eq. (2.9)):

$$E_{\max} = K_{1/2} \left( \frac{h_{\text{atm}} - h_1 - z_1}{z_1} \right) \quad (2.13)$$

where  $K_{1/2}$  is the average hydraulic conductivity ( $\text{cm d}^{-1}$ ) between the soil surface and the first node,  $h_{\text{atm}}$  is the soil water pressure head (cm) in equilibrium with the air relative humidity,  $h_1$  is the soil water pressure head (cm) of the first node, and  $z_1$  is the soil depth (cm) at the first node. Equation (2.13) excludes water flow due to thermal differences in the top soil and due to vapour flow, as on daily basis the concerned flow amounts are probably negligible compared to isothermal, liquid water flow (Koorevaar et al., 1983; Ten Berge, 1986; Jury et al., 1991). Note that the value of  $E_{\max}$  in Eq. (2.13) depends on the thickness of the top soil compartments. Increase of compartment thickness, generally results in smaller values for  $E_{\max}$  due to smaller hydraulic head gradients. For accurate simulations at extreme hydrological conditions, the thickness of the top compartments should not be more than 1 cm (see Par. 2.2.1).

There is one serious limitation of the  $E_{\max}$  procedure as described above.  $E_{\max}$  is governed by the soil hydraulic functions  $\theta(h)$  and  $K(\theta)$ . Still it is not clear to which extent the soil hydraulic functions, that usually represent a top layer of a few decimeters, are valid for the top few centimeter of a soil, which are subject to splashing rain, dry crust formation, root

extension and various cultivation practices. Therefore also empirical evaporation functions may be used, which require calibration of their parameters for the local climate, soil, cultivation and drainage situation. SWAP has the option to choose the empirical evaporation functions of Black (1969) or Boesten and Stroosnijder (1986).

Black calculated the cumulative actual evaporation during a drying cycle,  $\Sigma E_a$  (cm) as:

$$\sum E_a = \beta_1 t_{\text{dry}}^{1/2} \quad (2.14)$$

where  $\beta_1$  is a soil specific parameter ( $\text{cm d}^{-0.5}$ ), characterizing the evaporation process and  $t_{\text{dry}}$  is the time (d) after a significant amount of rainfall,  $P_{\text{min}}$ . SWAP resets  $t_{\text{dry}}$  to zero if the net precipitation  $P_{\text{net}}$  exceeds  $P_{\text{min}}$ .

<i>Model input</i>			
<i>Variable</i>	<i>Code</i>	<i>Description</i>	<i>Default</i>
$\beta_1$	COFRED	soil evaporation coefficient of Black ( $\text{cm d}^{-1/2}$ )	0.35
$P_{\text{min}}$	RSIGNI	Minimum amount of rainfall for reset Black time ( $\text{cm d}^{-1}$ )	0.5

The Black parameter  $\beta_1$  has been shown to be affected by  $E_p$  itself. In order to avoid this effect, Boesten and Stroosnijder (1986) proposed to use the sum of potential evaporation,  $\Sigma E_p$  (cm), as time variable:

$$\begin{aligned} \sum E_a &= \sum E_p & \text{for } \sum E_p &\leq \beta_2^2 \\ \sum E_a &= \beta_2 \left( \sum E_p \right)^{1/2} & \text{for } \sum E_p &> \beta_2^2 \end{aligned} \quad (2.15)$$

where  $\beta_2$  is a soil parameter ( $\text{cm}^{1/2}$ ), which should be determined experimentally. The parameter  $\beta_2$  determines the length of the potential evaporation period, as well as the slope of the  $\Sigma E_a$  versus  $(\Sigma E_p)^{1/2}$  relationship in the soil limiting stage.

For days with  $P_{\text{net}} < P_{\text{min}}$ , Boesten and Stroosnijder suggest the following procedure with respect to updates of  $\Sigma E_p$ . On days with no excess in rainfall ( $P_{\text{net}} < E_p$ ),  $\Sigma E_p$  follows from Eq. (2.15), that is:

$$\left( \sum E_p \right)^j = \left( \sum E_p \right)^{j-1} + \left( E_p - P_{\text{net}} \right)^j \quad (2.16)$$

in which superscript  $j$  is the day number.  $(\Sigma E_a)^j$  is calculated from  $(\Sigma E_p)^j$  with Eq. (2.15) and  $E_a$  is calculated with

$$E_a^j = P_{\text{net}}^j + \left( \sum E_a \right)^j - \left( \sum E_a \right)^{j-1} \quad (2.17)$$

On days of excess in rainfall ( $P_{\text{net}} > E_p$ )

$$E_a^j = E_p^j \quad (2.18)$$

and the excess rainfall is subtracted from  $\Sigma E_a$

$$\left( \sum E_a \right)^j = \left( \sum E_a \right)^{j-1} - \left( P_{\text{net}} - E_p \right)^j \quad (2.19)$$

Next  $(\Sigma E_p)^j$  is calculated from  $(\Sigma E_a)^j$  with Eq. (2.15). If the daily rainfall excess is larger than  $(\Sigma E_p)^{j-1}$ , then both  $(\Sigma E_a)^j$  and  $(\Sigma E_p)^j$  are set at zero.

<i>Model input</i>			
<i>Variable</i>	<i>Code</i>	<i>Description</i>	<i>Default</i>
$\beta_2$	COFRED	soil evaporation coefficient of Boesten/Stroosn. ( $\text{cm}^{1/2}$ )	0.54
$P_{\min}$	RSIGNI	Minimum amount of rainfall to reset sum $E_p$ ( $\text{cm d}^{-1}$ )	0.5

SWAP will determine  $E_a$  by taking the minimum value of  $E_p$ ,  $E_{\max}$  and, if selected by the user, one of the empirical functions. This procedure implicitly assumes that  $E_{\max}$  in general overestimates the maximum soil water flow near the soil surface.

## 2.2.4 Other boundary condition

The following other boundary conditions are taken into account:

- lateral boundary conditions (chapter 4);
- bottom boundary conditions (chapter 5);
- initial conditions.

Lateral and bottom boundary conditions are described elsewhere, respectively in chapters 4 and 5.

Initial conditions are implemented with 2 options:

- a) input of pressure heads for each compartment;
- b) input of a groundwater level. The nodal pressure heads will be calculated assuming hydrostatic equilibrium with the groundwater level, both in the saturated and unsaturated zone.

## 2.3 Soil hydraulic functions

The relationships between the water content  $\theta$ , the pressure head  $h$  and the hydraulic conductivity  $K$  are generally summarized in the retention function  $\theta(h)$  and the unsaturated hydraulic conductivity function  $K(\theta)$ . These soil hydraulic functions need to be specified for each distinct soil layer. An overview of measurement methods is given in Appendix 1.

Although tabular forms of  $\theta(h)$  and  $K(\theta)$  have been used for many years, currently analytical expressions are generally applied for a number of reasons. Analytical expressions are more convenient as model input and a rapid comparison between horizons is possible by comparing parameter sets. In case of hysteresis (Par. 6.2), scanning curves can be derived by some modification of the analytical function. Also scaling (Par. 6.3), which is used to describe spatial variability of  $\theta(h)$  and  $K(\theta)$ , requires an analytical expression of the reference curve. Another reason is to enable extrapolation of the functions beyond the measured data range. Last but not least, analytical functions allow for calibration and estimation of the soil hydraulic functions by inverse modeling.

Brooks and Corey (1964) proposed an analytical function of  $\theta(h)$  which has been widely used for a number of years. Mualem (1976) derived a predictive model of the  $K(\theta)$  relation based on the retention function. Van Genuchten (1980) proposed a more flexible  $\theta(h)$

function than the Brooks and Corey relation and combined it with Mualem's predictive model to derive  $K(\theta)$ . The Van Genuchten function has been used in numerous studies, forms the basis of several national and international data-bases (e.g. Carsel and Parrish, 1988; Yates et al., 1992; Leij et al., 1996; Wösten et al., 2001), and is implemented in SWAP.

The analytical  $\theta(h)$  function proposed by Van Genuchten (1980) reads:

$$\theta = \theta_{\text{res}} + \frac{\theta_{\text{sat}} - \theta_{\text{res}}}{\left(1 + |\alpha h|^n\right)^m} \quad (2.20)$$

where  $\theta_{\text{sat}}$  is the saturated water content ( $\text{cm}^3 \text{cm}^{-3}$ ),  $\theta_{\text{res}}$  is the residual water content in the very dry range ( $\text{cm}^3 \text{cm}^{-3}$ ) and  $\alpha$  ( $\text{cm}^{-1}$ ),  $n$  (-) and  $m$  (-) are empirical shape factors. Without losing much flexibility,  $m$  can be taken equal to :

$$m = 1 - \frac{1}{n} \quad (2.21)$$

Using the above  $\theta(h)$  relation and applying the theory on unsaturated hydraulic conductivity by Mualem (1976), the following  $K(\theta)$  function results:

$$K = K_{\text{sat}} S_e^\lambda \left[ 1 - \left( 1 - S_e^{\frac{1}{m}} \right)^m \right]^2 \quad (2.22)$$

where  $K_{\text{sat}}$  is the saturated conductivity ( $\text{cm d}^{-1}$ ),  $\lambda$  is a shape parameter (-) depending on  $\partial K / \partial h$ , and  $S_e$  is the relative saturation defined as:

$$S_e = \frac{\theta - \theta_{\text{res}}}{\theta_{\text{sat}} - \theta_{\text{res}}} \quad (2.23)$$

Van Genuchten et al. (1991) developed the program RETC to estimate the parameter values of this model from measured  $\theta(h)$  and  $K(\theta)$  data.

<i>Model input</i>			
<i>Specify for each soil layer:</i>			
<i>Variable</i>	<i>Code</i>	<i>Description</i>	<i>Default</i>
$\theta_{\text{res}}$	ORES	residual water content ( $\text{cm}^3 \text{cm}^{-3}$ )	0.01
$\theta_{\text{sat}}$	OSAT	saturated water content ( $\text{cm}^3 \text{cm}^{-3}$ )	
$\alpha$	ALFA	shape parameter of main drying curve ( $\text{cm}^{-1}$ )	
$n$	NPAR	shape parameter of main drying and main wetting curve (-)	
$K_{\text{sat}}$	KSAT	saturated hydraulic conductivity ( $\text{cm d}^{-1}$ )	
$\lambda$	LEXP	exponent hydraulic conductivity function (-)	0.5

## 2.4 Sink term: actual plant transpiration

The maximum possible root water extraction rate, integrated over the rooting depth, is equal to the potential transpiration rate,  $T_p$  ( $\text{cm d}^{-1}$ ), which is governed by atmospheric conditions (Chapter 3). The potential root water extraction rate at a certain depth,  $S_p(z)$  ( $\text{d}^{-1}$ ), may be determined by the root length density,  $\ell_{\text{root}}(z)$  ( $\text{cm cm}^{-3}$ ), at this depth as fraction of the integrated root length density (e.g. Bouten, 1992):

$$S_p(z) = \frac{\ell_{\text{root}}(z)}{\int_{-D_{\text{root}}}^0 \ell_{\text{root}}(z) dz} T_p \quad (2.24)$$

where  $D_{\text{root}}$  is the root layer thickness (cm).

SWAP can handle every distribution of  $\ell_{\text{root}}(z)$ . In practice this distribution is often not available. Therefore in many applications of SWAP, a uniform root length density distribution is assumed:

$$\frac{\ell_{\text{root}}(z)}{\int_{-D_{\text{root}}}^0 \ell_{\text{root}}(z) dz} = \frac{1}{D_{\text{root}}} \quad (2.25)$$

which leads to a simplified form of Eq. (2.24) (Feddes et al., 1978):

$$S_p(z) = \frac{T_p}{D_{\text{root}}} \quad (2.26)$$

Stresses due to dry or wet conditions and/or high salinity concentrations may reduce  $S_p(z)$ . The water stress in SWAP is described by the function proposed by Feddes et al. (1978), which is depicted in Figure 6.

Critical pressure head values of this sink term function are given in Appendix 3 (Taylor and Ashcroft, 1972). For salinity stress the response function of Maas and Hoffman (1977) is used (Figure 6), as this function has been calibrated for many crops (Maas, 1990). Appendix 4 lists salt tolerance data for a number of crops. It is still not clear if under the conditions where both stresses apply, the stresses are *additive* or *multiplicative* (Van Genuchten, 1987; Dirksen, 1993; Shalhevet, 1994; Homae, 1999). In order to simplify parameter calibration and data retrieval, we assume in SWAP the water and salinity stress to be multiplicative. This means that the actual root water flux,  $S_a(z)$  ( $\text{d}^{-1}$ ), is calculated from:

$$S_a(z) = \alpha_{\text{rw}} \alpha_{\text{rs}} S_p(z) \quad (2.27)$$

where  $\alpha_{\text{rw}}(-)$  and  $\alpha_{\text{rs}}(-)$  are the reduction factors due to water and salinity stresses, respectively.

Integration of  $S_a(z)$  over the root layer yields the actual transpiration rate  $T_a$  ( $\text{cm d}^{-1}$ ).

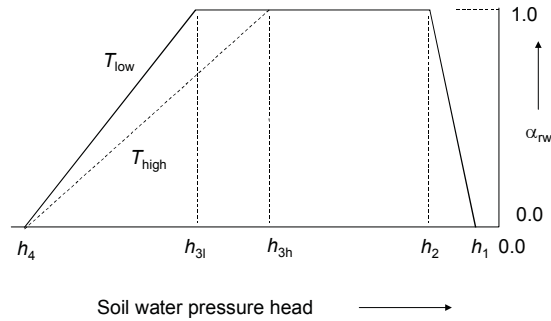


Figure 5 Reduction coefficient for root water uptake,  $\alpha_{rw}$ , as function of soil water pressure head  $h$  and potential transpiration rate  $T_p$  (after Feddes et al., 1978).

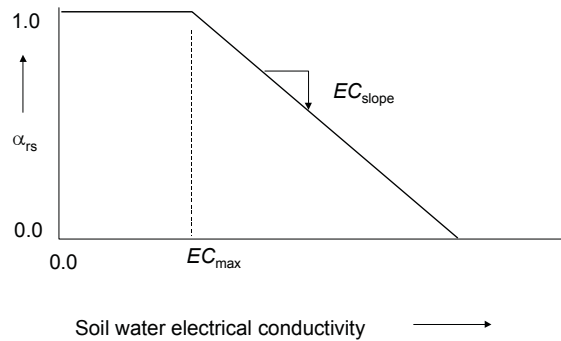


Figure 6 Reduction coefficient for root water uptake,  $\alpha_{rs}$ , as function of soil water electrical conductivity  $EC$  (after Maas and Hoffman, 1977).

**Model input**

Specify for each crop:

Variable Code	Description	Default	
$l_{root}$	RDENSITY	root length density as function of root depth	
$D_{root}$	RD	root depth as function of crop development stage (optional)	
$h_1$	HLIM1	no water extraction at higher pressure heads (cm)	
$h_2$	HLIM2U	h below which optimum water uptake starts for top layer (cm)	
$h_2$	HLIM2L	h below which optimum water uptake starts for sub layer (cm)	
$h_{3h}$	HLIM3H	h below which water uptake reduction starts at high $T_{pot}$ (cm)	
$h_{3l}$	HLIM3L	h below which water uptake reduction starts at low $T_{pot}$ (cm)	
$h_4$	HLIM4	Wilting point, no water uptake at lower pressure heads (cm)	
$T_{high}$	ADCRH	Level of high atmospheric demand ( $cm\ d^{-1}$ )	0.5
$T_{low}$	ADCRL	Level of low atmospheric demand ( $cm\ d^{-1}$ )	0.1
$EC_{max}$	ECMAX	$EC_{sat}$ level at which salt stress starts ( $dS\ m^{-1}$ )	
$EC_{slope}$	ECSLOPE	Decline of root water uptake above $EC_{max}$ ( $\% / dS\ m^{-1}$ )	

## 2.5 Frost conditions

The soil water freezes below a soil temperature of 0 °C. Optionally a frozen soil can be simulated, in which case the following parameters are directly adjusted:

- hydraulic conductivity  $K$ :

$$K^*(z) = f_T(z)(K(z) - K_{\min}) + K_{\min} \quad (2.28)$$

where  $K^*(z)$  is the adjusted hydraulic conductivity at depth  $z$  (cm d<sup>-1</sup>),  $K_{\min}$  is a very small hydraulic conductivity (cm d<sup>-1</sup>). For  $K_{\min}$  a default value is taken of 10<sup>-10</sup> cm d<sup>-1</sup>.

$f_T(z)$  is a correction factor for soil temperature at depth  $z$ , which is determined as:

$$\begin{aligned} f_T(z) &= \frac{T(z) - T_2}{T_1 - T_2} && \text{when } T_2 < T(z) < T_1 \\ f_T(z) &= 0 && \text{when } T(z) \leq T_2 \\ f_T(z) &= 1 && \text{when } T(z) \geq T_1 \end{aligned} \quad (2.29)$$

where  $T(z)$  is the soil temperature at depth  $z$  (°C),  $T_1$  is the soil temperature where reduction of hydraulic conductivity just begins (°C), and  $T_2$  is the soil temperature where reduction of hydraulic conductivity ends (°C). For  $T_1$  and  $T_2$  default values of 0.0 and -1.0 °C are taken.

- Pore volume in the soil  $V_{\text{air}}$  (cm) for a soil profile that becomes saturated:

$$V_{\text{air}} = \sum_{i=1}^m (\theta_{s,i} - \theta_i) \quad (2.30)$$

where  $\theta_s$  is the saturated water content (cm cm<sup>-3</sup>),  $\theta$  is the actual water content (cm cm<sup>-3</sup>),  $i$  is the number of the soil compartment and  $m$  is the number of soil compartments with a temperature below  $T_2$  starting to count from the top compartment. When a soil compartment is frozen ( $T(z) < T_2$ ) the pore volume of the total soil profile becomes smaller, because only the compartments above this layer are used in the calculation. An example is a soil in spring that is melting (Figure 7). The lower compartments were never frozen and the melting starts at the soil surface. It is possible that the first 4 compartments have melted and only the 5<sup>th</sup> is frozen. Now the pore volume is only calculated with the first 4 compartments.

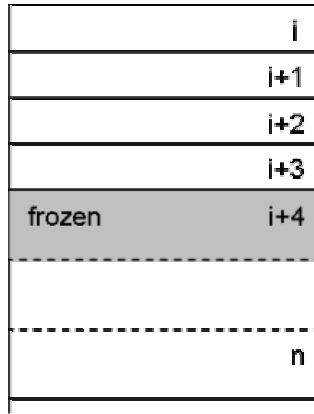


Figure 7 Partly frozen soil profile

- drainage fluxes of all drainage levels:

$$q_{drain,i}(z) = f_T(z) q_{drain,i}(z) \quad (2.31)$$

where  $q_{drain,i}(z)$  is the drainage flux at depth  $z$  from drainage level  $i$  ( $\text{cm d}^{-1}$ )

- bottom flux:

$$q_{bot} = f_T(z) q_{bot} \quad (2.32)$$

where  $q_{bot}$  is the flux across the bottom of the modelled soil profile

- actual crop uptake is reduced as:

$$S_a(z) = \alpha_f S_a(z) \quad \text{with} \quad \alpha_f = 0 \quad \text{when} \quad T(z) < 0 \text{ } ^\circ\text{C} \quad (2.33)$$

where  $\alpha_f$  is a multiplication factor for soil temperatures (-)

*Model input*

*Variable Code*

*Description*

- |           |  |
|-----------|--|
| - SWFROST | Switch, in case of frost: stop soil water flow, [Y=1, N=0] |
|-----------|--|